

VARIOUS ARTIFICIAL INTELLIGENCE ANALYSIS OF ATAXIC DISEASE PREDICTION BASED ON HUMAN GAIT RECOGNITION

¹PAVITHRA D S and ²SHRISHAIL MATH

¹Research Scholar, Visvesvaraya Technological University, Belgaum, Karnataka, India

²Professor, Computer Science and Engineering, Visvesvaraya Technological University, Belgaum, Karnataka, India

Abstract:

Ataxic gait monitoring and assessment of neurological disorders belong to important multidisciplinary areas that are supported by digital Image processing methods and machine learning tools. This paper presents the possibility of using image sensor data to optimize deep learning convolutional neural network systems to distinguish between ataxic and normal gait. The experimental dataset includes 4800 Images segments of 10 ataxic patients and 4 individuals from the control set with the mean age of 30 and 60 year, respectively. The proposed methodology is based upon the analysis of human gait images. The deep learning system uses all the Image components to extract the features using resent and to perform feature optimization. After selecting optimal features, classification of the ataxic or normal gait are done and then compared with standard methods, which include the MLP machine, Convolution neural network with features estimated as such as speed, step length, foot angle. Proposed result shows that the appropriate classification including increase in accuracy from 80% to 91.5% for the spine position. Combining the input data and the deep learning methodology with five layers the accuracy increases to 97.5%. Proposed methodology suggests that artificial intelligence methods and deep learning are efficient methods in the assessment of motion disorders, and they have a wide range of further applications.

Index Terms: Accelerometric signal analysis, computational intelligence, deep learning, classification, motion monitoring.

I. INTRODUCTION

Gait assessment and the study of motion disorders [1] – [5] have a wide range of applications in early diagnostics in neurology [6] – [8], physical therapy, rehabilitation, and physical activity analysis. The ataxic gait monitoring of patients with the multiple sclerosis forms a very important problem in this area. The recent rapid progress of sensor technology and wireless communication links allow the use of different micro electromechanical sensor units (MEMS), video, depth and thermal camera systems [9], [10], and wearable devices [11] – [15] for the associated motion analysis [16] – [19]. Specific mathematical methods are then used to process data in the time, frequency, or scale domains to perform human activity analysis.

This paper is devoted to the analysis of the gait patterns [20] that are related to ataxia [12], [21] – [24] as a neurological disorder associated with the loss of balance [6], [25].

The present analysis is based on three-axis accelerometric data of 16 ataxic patients and 19 healthy controls. All the datasets were acquired by a system of sensors located at different positions [8] of the body, using a full-body motion capture device (Perception Neuron [26]) to simultaneously record accelerometric data [27] during the gait. Computational intelligence and standard classification methods, including decision tree (DT), *k*-nearest neighbour (*k*-NN), support vector machines (SVM), Bayesian methods, and the two-layer neural network (NN) algorithms, are often used in this area [28]. All these methods assume the appropriate selection of features in the time, frequency and scale [29] domains.

Another more complex approach is based on the use of artificial intelligence and deep neural networks (DNNs) [30] – [35] that are applied to optimize multilayer mathematical systems and their coefficients. These methods are often used in the analysis of the body's motion [36], for the natural kinematics of human activity recognition [37] – [40], and for the evaluation of motion disorders. They allow us to avoid many of the problems related to feature selection and they are also used for more effective decision making in some cases. Although this complex approach [41], [42] to the construction of classification models can be very efficient, it needs sophisticated software and powerful computational tools.

The goal of the present study is to contribute to the analysis of accelerometric data for motion monitoring and to compare the results of the deep learning with further classification methods for the recognition of different motion patterns associated with an ataxic gait. From the more general point of view, it contributes to the classification of motion disorders in neurology. It also allows us to improve the treatment outcomes and to reduce the need for invasive procedures. The results point to the use of artificial intelligence methods in human activity monitoring and motion analysis in different areas.

Machine learning Algorithms:

With the increased usage of technology, data collection has been easier in different disciplines including medicine, business, education, security and so on. Automatic visual surveillance is of paramount importance due to security problems in recent years. Cameras provide potential sources for capturing data useful for gait recognition. Gait recognition is among the most appropriate biometric methods. Moreover, the development of open source

and commercial machine learning and data mining tools enabled experts to employ systems to support decisions on these data collected in different fields.

Machine learning is a way of automation that studies the structure and function of algorithms that can learn and make estimations based on the given data. Such

algorithms work by constructing a model to perform data-driven estimates and decisions from sample inputs rather than strictly following static program instructions. It is a paradigm that makes inferences from existing data using mathematical and statistical models and makes predictions about the unknown with these inferences. There are three types of learning techniques: supervised learning, unsupervised learning, and reinforcement learning.

Supervised Learning: This is the learning process of inferring a function from labeled/tagged observations (training data). In supervised learning, the learning algorithm infers a function during the training phase by mapping the training data instance

to its corresponding label. For example, if an “unknown user” asks for “personal information” in a mail, this is classified as a spam.

Unsupervised Learning: This is the learning process from unlabeled observations. The algorithm is expected to make self-discoveries and model probability densities of given inputs without labels (training data). For example, discovering the probability density of “unknown users” and the phrase “personal information”.

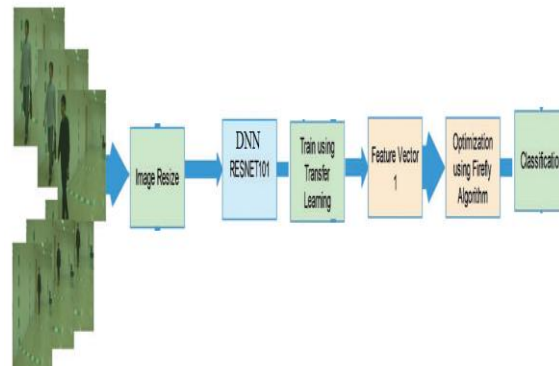
Reinforcement Learning: This is the learning process based on data where the learning algorithm learns to take action in an environment (training data) to maximize some notion of cumulative reward. These type of learning problems assume the existence of temporal information.

In this work, machine learning of particular interest to us is required to discover spatial patterns in sensor data. To this end, we are using the two basic types of machine learning supervised and unsupervised. In this research, we have a feature vector of biometric measurements (gait data) and we aim to explore whether they are informative enough to identify a specific person. In order to make the identification either the biometric is sufficiently unique that clustering (distance calculation) relative to the original feature space will be sufficient, or a mapping from feature to label space is necessary (classification). In the following, we discuss the machine learning algorithms used in this research.

II. Proposed Methodology

This section describes the proposed human gait recognition method. Depicts the main flow diagram of the proposed approach. Pre-processing datasets, feature extraction using pretrained models, feature optimization, and classification are the main steps in this method. Deep transfer learning is used to modify two pre-trained models, Resnet. The features are then extracted from modified model. We get resultant vectors as a

result, which are then optimized using improved ant colony optimization (ACO). Finally, the final features are classified using multiclass classification methods.



Dataset Collection:

CASIA B [24] is a large multiview gait dataset that was created in January of 2005. 20 subjects are involved in the collection of this dataset. The dataset was captured by all subjects using the 4 different view angles. This dataset includes three deviations: changes in view angle, changes in clothing, and changes in carrying objects. This dataset contains three classes: walk with a bag, normal walk, and walk with front. We consider three angles in this work: 0, 18, and 180. Three conditions are included for each angle: bag carrying, normal walking.

Figure shows a few examples of images from this dataset.

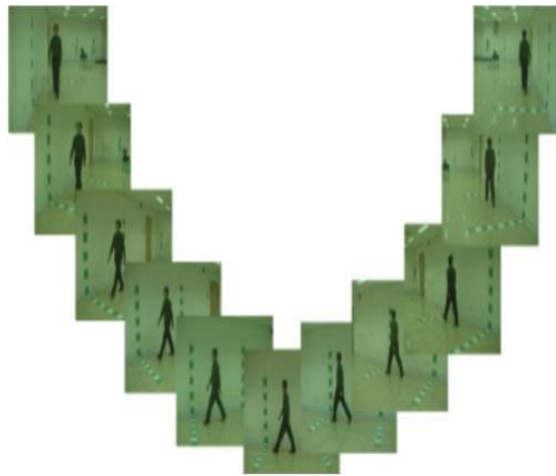


Figure: Sample CASIA B dataset

MLP classifier:

Artificial neural networks are nonlinear information processing devices which are built from interconnected processing devices called “neurons”. It is an interconnected group of artificial neurons that uses a mathematical model or computational model for information. ANN is inspired by the way biological neural system works. The neural network is trained using the image data and the trained neural network is capable to identify a person. Back propagation is a systematic method for training multi-layer artificial neural networks. It is a multi-layer forward network using extend gradient descent based delta learning rule, commonly known as Back propagation rule. Back propagation provides a computationally efficient method for changing the weights in a feed forward network with differentiable activation function units to learn a training set of input-output examples. Being a gradient descent method it minimizes the total squared error of the output computed by the net. The network is trained by supervised learning method. A multilayer perceptron (MLP) is a feed forward artificial neural network model that maps sets of input data onto a set of appropriate outputs. A MLP consists of multiple layers of nodes with each layer fully connected to the next one. MLP utilizes a supervised learning technique called back propagation for training the network. MLP is a modification of the standard linear perceptron and can distinguish data that are not linearly separable. The multilayer perceptron consists of three or more layers (an input and an output layer with one or more hidden layers) of nonlinearly-activating nodes and is thus considered a deep neural network. Each node in one layer connects with a certain weight to every node in the following layer. Learning occurs in the perceptron by changing connection weights after each piece of data is processed, based on the amount of error in the output compared to the expected result. This is supervised

learning, and is carried out through back propagation, a generalization of the least mean squares algorithm in the linear perceptron. Learning rate is carefully selected to ensure that the weights converge to a response fast enough, without producing oscillations.

Convolutional Neural Network (CNN):

Deep learning demonstrated massive success in the classification phase of machine learning [25,26]. The convolutional neural network (CNN) is a deep learning technique. Using a convolutional operator, image pixels are convolved into features in this network. It aids us in image recognition, classification, and object detection. When compared to other classification algorithms, it requires very little pre-processing. CNN uses an image as input and then processes it through the hidden layers to classify it. The training and testing process will go through several layers, including a convolutional layer, a pooling layer, an activation layer, and a fully connected layer.

Convolutional Layer

Suppose we have some $P \times P$ filter neuron in the layers. Consider, we have $n \times n$ filter ω ; then the convolutional layer has an output of $(P-n+1) \times (P-n+1)$. To calculate the pre-nonlinearity

input to some unit x_{ij}^l in the layer, it is defined as follows:

$$x_{ij}^l = \sum_{a=0}^{n-1} \sum_{b=0}^{n-1} \omega_{ab} y_{(i+a)(j+b)}^{l-1}$$

ReLU Layer

ReLU layer is an activation layer used for the problem of non-linearity among layers. Through this layer, the negative features are converted into zero values. Mathematically, it is defined as follows:

$$f(x) = \max(0, x)$$
$$f(x) = \begin{cases} 0, & \text{if } x < 0 \\ x, & \text{if } x \geq 0 \end{cases}$$

Batch Normalization

The batch normalization is achieved through the normalization step that fixes each of the inputs layer's means and variances. Ideally, the normalization will be conducted on the entire training set. Mathematically, it is formulated as follows:

$$\mu_B = \frac{1}{m} \sum_{i=1}^m x_i \quad \text{and} \quad \sigma_B^2 = \frac{1}{m} \sum_{i=1}^m (x_i - \mu_B)^2$$

where B denotes the mini-batch of the size m of the whole training set.

Pooling Layer

The pooling layer is normally applied after the convolution layer to reduce the spatial size of the input. It is applied individually to each depth slice of an input volume. The volume depth is always conserved in pooling operations. Consider, we have an input volume of the width W^1 , height H^1 , and depth D^1 . The pooling layer requires the two hyper-parameters such as kernel/filter size G and stride Z . On applying the pooling layer on the input volume, the output dimensions of output will be as:

$$W^2 = (W^1 - G)/Z + 1$$

$$H^2 = (H^1 - G)/Z + 1$$

$$D^2 = D^1$$

Average Pooling Layer

The average pool layer calculates the average value for each patch on a feature map. Mathematically, it is formulated as follows:

$$s_j = \lambda \max_{i \in R_j} a_j + (1 - \lambda) \frac{1}{|R_j|} \sum_{i \in R_j} a_i$$

where λ decides to use either max pooling or average pooling, the value of λ is selected randomly in either 0 or 1. When $\lambda = 0$, it behaves like average pooling, and when $\lambda = 1$, it works like max pooling.

Fully Connected Layer

Neurons in the fully connected layer (FC) have full connections to all the activations in the previous layer. The activations can later be computed with the matrix multiplication followed by the bias offset. Finally, the output of this layer is classified using Softmax classifier for the final classification. Mathematically, this function is defined as follows:

$$\sigma(\vec{z})_i = \frac{e^{z_i}}{\sum_{j=1}^K e^{z_j}}$$

where, \vec{z} denotes the input vector to a Softmax function made up of (z_0, \dots, z_K) . All the values of z_i are used as input to a softmax function, and it can take any positive, zero, or negative real value. The exponential function is applied to each value as the input vector.

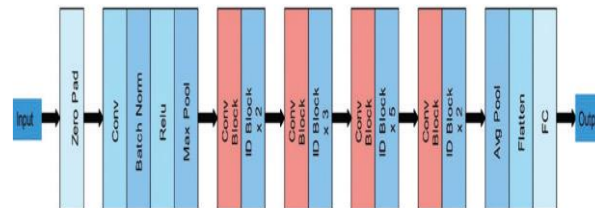
Deep Learning Features:

In the literature, several models are introduced for classification, such as ResNet, VGG, GoogleNet, InceptionV3, and named a few more [27]. In this work, we utilized two pre-trained deep learning models-ResNet101. The detail of each model is given as follows.

Modified ResNet

ResNet represents the residual network, and it has a significant part in computer vision issues. ResNet101 [28] contains 104 convolutional layers comprised of 33 blocks of layers, and 29 of these squares are directly utilized in previous blocks. Initially, this network was trained on the ImageNet dataset, which includes 1000 object classes. The original architecture has been illustrated in figure. This figure demonstrated that the input images are processed in residual blocks, and each block consists of several layers. In this work, we modify this model and remove the FC layer, which includes 1000 object classes. We added a new FC layer according to our number of classes. In our selected dataset, the number of classes is three, such as normal walk, walking with carrying a bag, and walking with a coat. The input size of the modified model is consistent as $224 \times 224 \times 3$, and output is $N \times 3$. The modified model is illustrated in Fig. This figure shows that this modified model consists of a convolution layer, max pooling layer with the stride of 2, 33 residual building blocks, avg pooling layer with the stride of 7, and a new fully-connected layer.

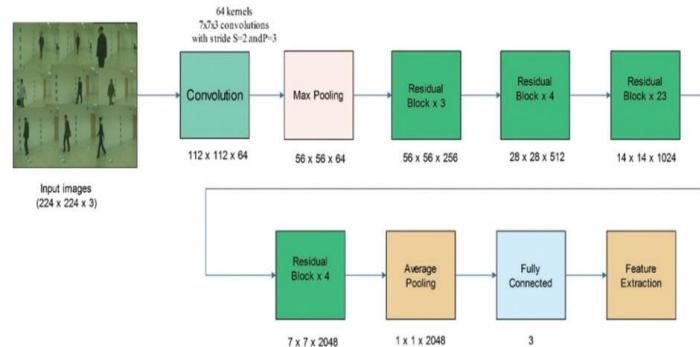
After this, we trained this modified model using transfer learning (TL) [29,30]. TL is a process of reuse a model for a new task. Mathematically, it is formulated as follows:



(m, n) is the training data sizes where n_m and $\rho D 1$ and $\rho T 1$ be the labels of training data. Then the TL is represented as:

$$DS = DT, LD = LT$$

Visually, this process is illustrated in Fig. This figure describes that the weights of original models are transferred to the new modified model for training. From the modified model, features are extracted from the feature layers of dimension $N \times 2048$



Features Optimization

Optimal feature selection is an important research area in pattern recognition [32,33]. Many techniques are presented in the literature for features optimization, such as PSO, ACO, GA, and name a few more. We proposed an algorithm for feature selection named improved ant colony optimization (ACO) in this work. The working of the original ACO [34] is given as follows:

Starting Ant Optimization—The number of ants are computed as follows at the very first step:

$$A_N = \sqrt{F \times W}$$

where F represents the input feature vector, w represents the width of a feature vector, and AN denotes the total number of ants used for the random placement in the entire vector, where each feature in the vector represents one ant.

Decision-Based on probability—The probability of the ant traveling is represented by p_{ij} through pixel (e, f) to pixel (g, h) . The probability can be computed as follows:

$$p_{ef} = \frac{(p_{ef})(p_{ef})^a}{\sum (p_{ef})^a (w_{ef})^a u_{ef}(\Delta)}$$

Here, every feature location is given as $e, f \in _$. The p_{ef} shows the number of pheromones, w_{ef} represents the visibility, and its value is explained with the help of the

$$w_{ef} = H_{ef}$$

$$\Delta = 0, \pi/4, \pi/2, 3\pi/4, \pi$$

following function:

Rules of Transition—This rule is mathematically present as follow:

$$S = \{arg \{max_j \in Q[(\rho_{ij})^a (w_{ij})^a bu_{ij}(\Delta)]\}\}, \quad \text{when } q < q_0$$

Here, i, j represent the locations of each feature, and these pixels are traveling to a location (k, l) . If $q < q_0$ the next pixel that the ants would visit is chosen as shown in the second part's probability distribution. **Pheromone Update**—In this step, the ants are shifted from the i, j to update features location (k, l) . Based on this, the path of pheromone is obtained after every iteration and mathematically

defined as follow:

$$\rho_{ij} = (1 - \eta) \cdot \rho_{ij} + \eta \cdot \Delta \rho_{ij}$$

$$\Delta \rho_{ij} = w_{ij}$$

Here, η ($0 < \eta < 1$) shows the ratio of loss of pheromones. A new value of pheromones is obtained after every iteration. Mathematically, this process is formulated as follow:

$$\rho_{ij} = (1 - \theta) \cdot \rho_{ij} + \theta \cdot \rho_0$$

Here, $\theta(0 < \theta < 1)$ shows the promotions of loss pheromones. New values of pheromones and ρ_0 represents the start values of pheromones. These steps are applied for all features, and in the output, we obtained an optimal feature vector. The number of iterations in this work was 100. After 100 iterations, the selected vector is obtained of dimensions $N \times 800$ and $N \times 750$, respectively. These vectors are obtained for both modified model ResNet. We found some redundant features in these selected vectors during the analysis step, which affects the recognition accuracy. Therefore, we modify this method by adding one new equation.

Mathematically, it is formulated as follows:

$$Act = \begin{cases} F_{sel}(i) & \text{for } F_i \geq \bar{\sigma} \\ Discard, & \text{Elsewhere} \end{cases}$$

$$\bar{\sigma} = \frac{\mu + \sigma^2}{\sigma}$$

$$\mu = \frac{1}{N} \sum_{i=1}^K (F_i), \quad \sigma^2 = \frac{\sum (F_i - \bar{F})^2}{N-1}, \quad \sigma = \sqrt{\sigma^2}$$

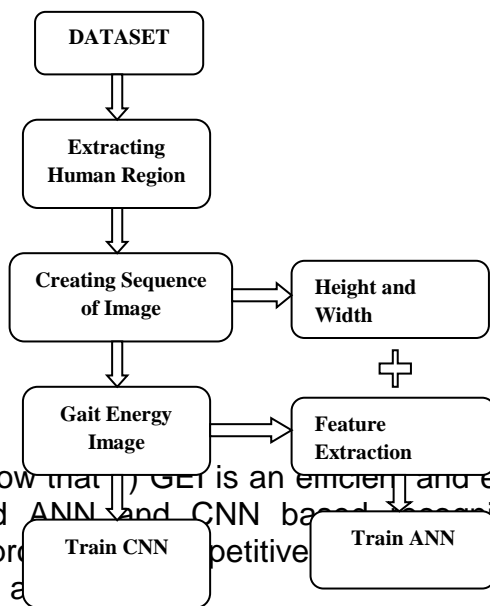
Here, *Act* represent the activation function which selects or discard the features based on the . In this step, 20%–30% of features are further removed. Based on the analysis step, we found the selected features better and utilized them for the final classification (in this work, the final feature vector size is $N \times 1150$). The classification is conducted through multiple classifiers and chooses the best of them based on the accuracy value.

III. Experimental Results and Analysis:

In the beginning, the proposed statistical feature fusion approach is described for gait-based human recognition. One by one video Silhouette image will be read from dataset and person location from image will be extracted and reshaped to 300 by 100. Before resizing the person, height and width value will be stored, then from sequence of human image Gait energy image (GEI) will be formed and following feature will be extracted: average of height, width, mean, standard deviation, variance. Once person region extracted, leg region of person will be obtained, and GEI will be created then from that above feature will be extracted and combined with the previous feature that are

extracted for complete body region. With these features, Artificial Neural Network (ANN) will be trained.

And with the GEI image, Convolutional Neural Network (CNN) is trained, and the result of both ANN and CNN is compared.



Test results show that 1) GEI is an efficient and effective gait representation and 2) we have proposed ANN and CNN based gait recognition approach among of that CNN accomplishes more competitive results with respect to the published major gait recognition approaches.

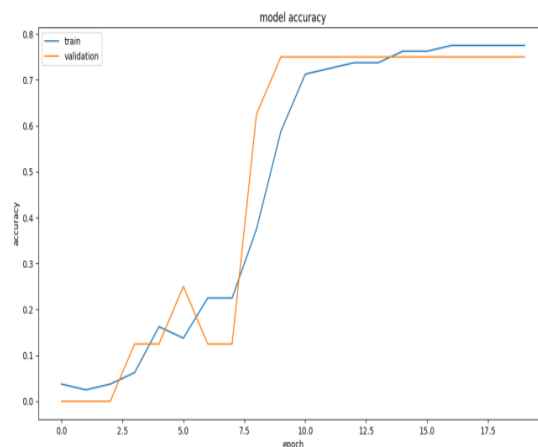


Figure: CNN Training and Validation Accuracy

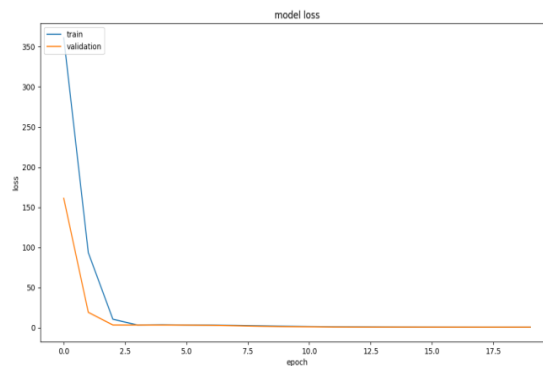


Figure: CNN Training Validation Loss

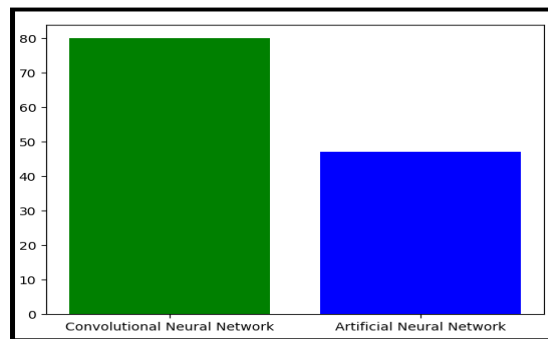


Figure: Accuracy plot of CNN vs ANN

The experimental process such as experimental setup, dataset, evaluation measures, and results is discussed in this section. The CASIA B dataset is utilized in this work and divide into 70:30. Its means that 70% dataset is used for the training purpose and the remaining 30% data for testing. During the training process, we initialized epoch's 200, iterations 300; mini-batch size is 32 and learning rate 0.0001. For learning, the Stochastic Gradient Descent (SGD) optimizer is employed. For the cross-validation, the ten-fold process was conducted. Multiple classifiers are used, and each classifier is validated by six measures such as recall rate, precision, accuracy, and name a few more. All the simulation of this work is conducted in Python IDE 3.7.

Three different persons are considered for the experimental process. The results are computed for modified deep models such as ResNet. For all four angles, the results of the ResNet model are presented. These tables show that the DCNN performed well using the proposed method for all three selected angles.

The results of 0 angles and achieved the best accuracy of 95.2%. The recall rate and precision rate of this DCNN is 97.5%.

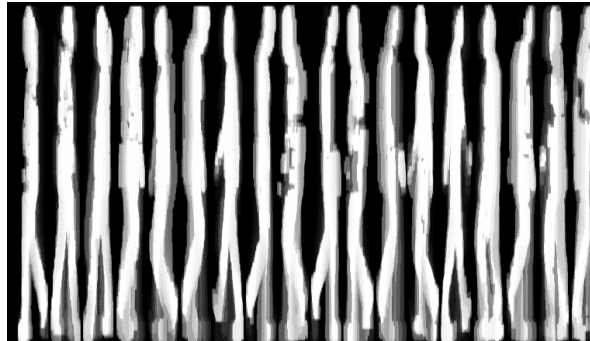
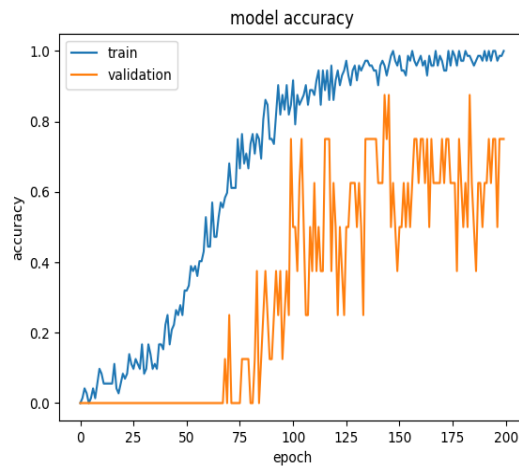


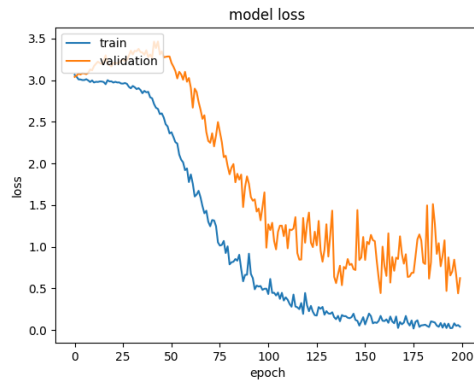
Table: Accuracy of classifiers

S.No	Accuracy in %
MLP classifier	42.50%
CNN classifier	94.90%
Proposed DCNN	97.50%

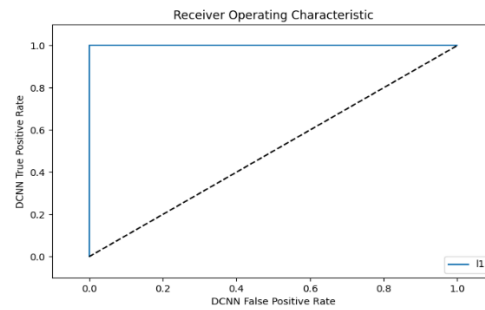
DCNN model Accuracy:



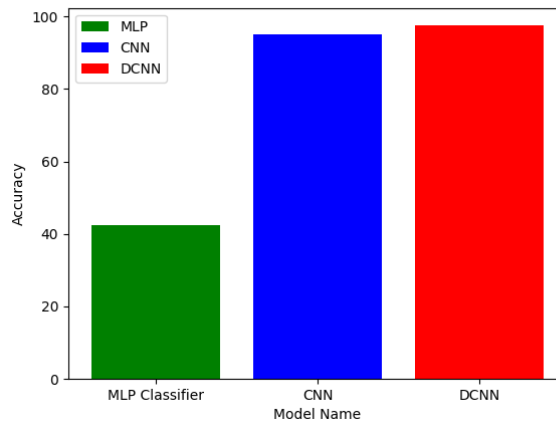
DCNN model Loss:



ROC curve of Proposed Method:



Comparison of Existing Work:



IV. Conclusion

First, a brief discussion of the results section has been added to analyze the proposed framework. The results show that the proposed framework performed well on the chosen dataset. The accuracy of 0 and 180 degrees is better for modified ResNet and ACO. When compared to CNN, the computational cost is lower. Furthermore, the original computational cost of ResNet is nearly three times that of the proposed framework (applying after the ACO). Table 1 also includes a fair comparison with the most recent techniques. In this table, it is demonstrated that the proposed accuracy outperforms the existing techniques. Based on the results, we can conclude that the ACO aids in improving recognition accuracy while also reducing computational time. Because the accuracy of improved deep model is insufficient and falls short of recent techniques, we proposed an ACO algorithm. The choice of a deep model is the main limitation of this work because we consider model.

References

1. Bera, D. Bhattacharjee and H. P. Shum, "Two-stage human verification using HandCAPTCHA and anti-spoofed finger biometrics with feature selection," *Expert Systems with Applications*, vol. 171, pp. 114583, 2021.
2. M. Hassaballah and K. M. Hosny, "Recent advances in computer vision," in *Studies in Computational Intelligence*, vol. 804. Cham: Springer, pp. 1–84, 2019.
3. S. Kadry, P. Parwekar, R. Damaševičius, A. Mehmood, J. Khan *et al.*, "Human gait analysis for osteoarthritis prediction: A framework of deep learning and kernel extreme learning machine," *Complex and Intelligent Systems*, vol. 8, pp. 1–21, 2021.
4. M. Sharif, M. Z. Tahir, M. Yasmim, T. Saba and U. J. Tanik, "A machine learning method with threshold based parallel feature fusion and feature selection for automated gait recognition," *Journal of Organizational and End User Computing*, vol. 32, pp. 67–92, 2020.
5. K. Javed, S. A. Khan, T. Saba, U. Habib, J. A. Khan *et al.*, "Human action recognition using fusion of multiview and deep features: An application to video surveillance," *Multimedia Tools and Applications*, vol. 9, pp. 1–27, 2020.
6. Y.-D. Zhang, S. A. Khan, M. Attique, A. Rehman and S. Seo, "A resource conscious human action recognition framework using 26-layered deep convolutional neural network," *Multimedia Tools and Applications*, vol. 11, pp. 1–23, 2020.
7. M. Hassaballah, M. A. Hameed, A. I. Awad and K. Muhammad, "A novel image steganography method for industrial internet of things security," *IEEE Transactions on Industrial Informatics*, vol. 1, pp. 1–8, 2021.
8. H. Arshad, M. Sharif, M. Yasmin and M. Y. Javed, "Multi-level features fusion and selection for human gait recognition: An optimized framework of Bayesian model and binomial distribution," *International Journal of Machine Learning and Cybernetics*, vol. 10, pp. 3601–3618, 2019.

9. R. Liao, S. Yu, W. An and Y. Huang, "A model-based gait recognition method with body pose and human prior knowledge," *Pattern Recognition*, vol. 98, pp. 107069, 2020. CMC, 2022, vol.70, no.2 2129
10. S. Shirke, S. Pawar and K. Shah, "Literature review: Model free human gait recognition," in *2014 Fourth Int. Conf. on Communication Systems and Network Technologies*, NY, USA, pp. 891–895, 2014.
11. X. Wang and W. Q. Yan, "Human gait recognition based on frame-by-frame gait energy images and convolutional long short-term memory," *International Journal of Neural Systems*, vol. 30, pp. 1950027, 2020.
12. M. Kumar, N. Singh, R. Kumar, S. Goel and K. Kumar, "Gait recognition based on vision systems: A systematic survey," *Journal of Visual Communication and Image Representation*, vol. 4, pp. 103052, 2021.
13. M. Deng, T. Fan, J. Cao, S.-Y. Fung and J. Zhang, "Human gait recognition based on deterministic learning and knowledge fusion through multiple walking views," *Journal of the Franklin Institute*, vol. 357, pp. 2471–2491, 2020.
14. Tarun and A. Nandy, "Human gait classification using deep learning approaches," in *Proc. of Int. Conf. on Computational Intelligence and Data Engineering*, NY, USA, pp. 185–199, 2021.
15. M. Sharif, T. Akram, M. Raza, T. Saba and A. Rehman, "Hand-crafted and deep convolutional neural network features fusion and selection strategy: An application to intelligent human action recognition," *Applied Soft Computing*, vol. 87, pp. 105986, 2020.
16. Sharif, K. Javed, H. Gulfam, T. Iqbal, T. Saba *et al.*, "Intelligent human action recognition: A framework of optimal features selection based on Euclidean distance and strong correlation," *Journal of Control Engineering and Applied Informatics*, vol. 21, pp. 3–11, 2019.
17. M. S. Sarfraz, M. Alhaisoni, A. A. Albeshir, S. Wang and I. Ashraf, "Stomachnet: Optimal deep learning features fusion for stomach abnormalities classification," *IEEE Access*, vol. 8, pp. 197969 – m197981, 2020.
18. N. Hussain, A. Majid, M. Alhaisoni, S. A. C. Bukhari, S. Kadry *et al.*, "Classification of positive COVID-19 CT scans using deep learning," *Computers, Materials and Continua*, vol. 66, pp. 1–15, 2021.
19. M. Rashid, M. A. Khan, M. Alhaisoni, S.-H. Wang, S. R. Naqvi *et al.*, "A sustainable deep learning framework for object recognition using multi-layers deep features fusion and selection," *Sustainability*, vol. 12, pp. 5037, 2020.
20. Mehmood, S. A. Khan, M. Shaheen and T. Saba, "Prosperous human gait recognition: An end-to-end system based on pre-trained CNN features selection," *Multimedia Tools and Applications*, vol. 11, pp. 1–21, 2020.
21. R. Anusha and C. Jaidhar, "Clothing invariant human gait recognition using modified local optimal oriented pattern binary descriptor," *Multimedia Tools and Applications*, vol. 79, pp. 2873–2896, 2020.
22. H. Arshad, M. I. Sharif, M. Yasmin, J. M. R. Tavares, Y. D. Zhang *et al.*, "A multilevel paradigm for deep convolutional neural network features selection with an application to human gait recognition," *Expert Systems*, pp. e12541, 2020.
23. K. Sugandhi, F. F. Wahid and G. Raju, "Statistical features from frame aggregation and differences for human gait recognition," *Multimedia Tools and Applications*, vol. 18, pp. 1–20, 2021.
24. S. Zheng, J. Zhang, K. Huang, R. He and T. Tan, "Robust view transformation model for gait recognition," in *2011 18th IEEE Int. Conf. on Image Processing*, NY, USA, 2011, pp. 2073–2076.
25. Y.-D. Zhang, M. Sharif and T. Akram, "Pixels to classes: Intelligent learning framework for multiclass skin lesion localization and classification," *Computers & Electrical Engineering*, vol. 90, pp. 106956, 2021.

26. T. Akram, Y.-D. Zhang and M. Sharif, "Attributes based skin lesion detection and recognition: A mask RCNN and transfer learning-based deep learning framework," *Pattern Recognition Letters*, vol. 143, pp. 58–66, 2021.
27. F. Emmert-Streib, Z. Yang, H. Feng, S. Tripathi and M. Dehmer, "An introductory review of deep learning for prediction models with big data," *Frontiers in Artificial Intelligence*, vol. 3, pp. 4, 2020.
28. Y. Rao, L. He and J. Zhu, "A residual convolutional neural network for pan-sharpening," in *2017 Int. Workshop on Remote Sensing with Intelligent Processing*, Toronto, Canada, pp. 1–4, 2017.
29. T. Kaur and T. K. Gandhi, "Deep convolutional neural networks with transfer learning for automated brain image classification," *Machine Vision and Applications*, vol. 31, pp. 1–16, 2020.